Catalytic Activity and Kinetic Studies of Core@Shell Nanostructure Cu/Zn Ferrite @Al_2O_3, CuO for Degradation of Para-Nitro Phenol

Sannan Salabat Butt
Department of Energy and Environmental Engineering, Interdisciplinary Graduate School of Engineering Sciences, Kyushu University

Pervaiz, Erum
Department of Chemical Engineering, School of Chemical & Materials Engineering (SCME), National University of Sciences and Technology (NUST)

https://doi.org/10.5109/5909120

出版情報：Proceedings of International Exchange and Innovation Conference on Engineering & Sciences (IEICES). 8, pp.373-379, 2022-10-20. Interdisciplinary Graduate School of Engineering Sciences, Kyushu University
バージョン：

Proceedings of the 8th International Exchange and Innovation Conference on Engineering & Sciences (IEICES 2022)

Catalytic Activity and Kinetic Studies of Core@Shell Nanostructure Cu/Zn Ferrite @Al_2O_3, CuO for Degradation of Para-Nitro Phenol

Sannan Salabat Butt [1,2*], Erum Pervaiz [2*]
[1] Department of Energy and Environmental Engineering, Interdisciplinary Graduate School of Engineering Sciences, Kyushu University, 6-1 Kasuga-koen, Kasuga-shi, Fukuoka 816-8580, Japan,
[2] Department of Chemical Engineering, School of Chemical & Materials Engineering (SCME), National University of Sciences and Technology (NUST), Islamabad, Pakistan
*Corresponding authors emails: butt.sannan.445@s.kyushu-u.ac.jp, erum.pervaiz@scme.nust.edu.pk

Abstract: *Current research focuses on the synthesis of magnetically separable core@shell nanoparticles of Cu/Zn Ferrite /Al_2O_3, CuO for Degradation of Para-Nitro Phenol. The cores were synthesized using the hydrothermal method while the nanoparticles obtained were coated with CuO and Al_2O_3 using the co-precipitation method. The synthesized nanostructures were characterized for structural and morphological behavior using XRD and SEM. Spinel crystal structure and coating were confirmed from the characteristic peaks in the indexed XRD patterns whereas SEM images show the uniform particle size distribution. The synthesized nano-catalysts were applied for the reduction of Para-nitro phenol with excess sodium borohydride. As evidenced by the UV spectra, all the 6X synthesized nano-catalyst were found as active catalysts, with $ZnFe_2O_4$@CuO having a maximum catalytic conversion of 80.00%.*

Keywords: Core-shell nanostructures, CuO/Al_2O_3 coating, Magnetic nanoparticles, Spinel ferrites

6. INTRODUCTION

With the rapid growth of industrialization, there is a tremendous increase in the release of hazardous pollution. It has created serious pollution mainly from the textile, paint, oil, and medicines industry. Dangerous pollutants contain many aromatic nitro compounds and phenol [1]. Core-shell nano ferrites may be useful in the degradation of aromatic nitro compounds into less dangerous components. There are different types of aromatic nitro compounds [2]. Nitrophenol is one of the major pollutants among the various aromatic nitro compounds, nitrophenol is considered the most harmful pollutant [3]. It is one of the main pollutants in agricultural and industrial wastewater. Its high toxicity and harmful nature have enlisted it among the most harmful pollutants by the Environmental Protection Agency (EPA) in the United States. Nitrophenol is a very harmful pollutant as they become persistent in the environment, and they are not biodegradable. It is very important to remove or reduce this nitrophenol from sewage otherwise it can severely affect aquatic life [4].

Nitrophenol is a stable compound and is not easily reduced. Therefore, it is required to develop a catalyst that can be used to easily reduce nitrophenol. The main idea behind the study is to improve engineering operations and take advantage of nanotechnology to develop an effective catalyst. The synthesis and the use of an effective catalyst are to make industrial processes more efficient.

Ferrites are ceramic compound that comprises stable electrical, mechanical, and chemical properties. Nowadays they are used in the development of active electronic devices, computer chips, and biomedical applications. Spinel ferrites can also be used as catalyst spinel ferrites [5].

The present study focuses on the synthesis of spinel ferrites, coating the ferrite with shell and using them as a catalyst. A total of three core nanostructures are prepared by hydrothermal process. They were then individually coated with cupric oxide and alumina by using a co-precipitation process. Making a total of six core/ shell, nanostructures.

The main objectives of the present study are mentioned below:

I. Synthesis of cupric oxide & alumina coated Nanoparticles.
II. Structural and morphological analysis by X-Ray Diffraction (XRD), Scanning Electron Microscopy (SEM).
III. Performing kinetic and catalytic study using UV spectroscopy.

A brief review of different ways to prepare nanoparticles is given along with characterization tools, which are commonly used for the physical and chemical analysis of these nanoparticles. The different synthesis methods are illustrated in Figure 1.

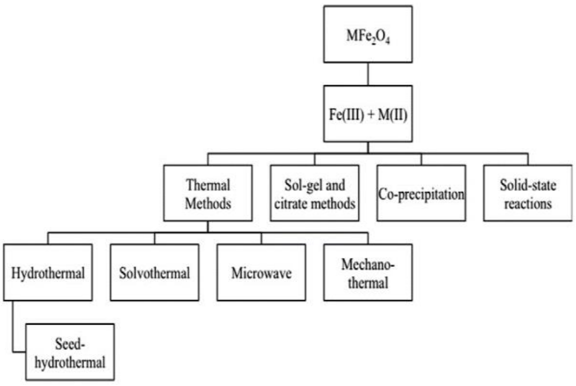

Fig. 1. Preparation methods of ferrites using Fe (III) and M (II) salt as precursors [5]

6.1 Synthesis of Core/shell Structure

The synthesis of magnetic ferrite is of great interest to researchers and scientists because of the great effectiveness of applications in the nanometer size range and in different scientific and engineering fields. They have a complex composition, and they can be used in the fields of electronics, nano catalysis, and biomedicine.

There are two ways to synthesize Nano sized particles [6] The method names are as follows

I. Top-down approach

II. Bottom-up approach

In the top-down approach, the particles in the nano-size range are synthesized from bulk material or large-sized particles. The "bottom-up" approach contradicts the top-down approach involving the "synthesis of nanoparticles with atomic-level control." The bottom-up approach involves building materials from the bottom: atom by atom and molecule by molecule. Common examples of such methods are hydrothermal process, thin film deposition, co-precipitation, and sol-gel processes [7].

1.2 Methods for the synthesis of Spinel Ferrites

There are two methods that are employed for the synthesis of nano-sized ferrites.

I. Dry Methods
II. Wet chemical Methods

1.2.1 Dry Methods:

The dry method follows a top-down process for the synthesis of Nanosized ferrite. The dry process can be solid state reaction, grinding, and milling. This is an old technique for preparing nanosized ferrite. Solid state reactions are the old techniques used to synthesize ferrite. The technique involves the direct addition of the reagent oxide and then the treatment of the mixing agent at a higher temperature for about 8 to 12 hours. This method is used when mass production is required, as well as a wide range of particle size distributions. This requires higher energy. [7]

In the dry process, it is difficult to control the size & morphology of the nano-sized ferrite. Other methods, such as attrition, cutting, or grinding, also follow the top-down approach to synthesizing ferrite. It involves multiple mechanical cycles and creates problems of the large size distribution (10 nm to 100 nm).

1.2.2 Wet Chemical Methods:

Wet chemical methods follow a bottom-up approach. Wet chemical methods are more effective and efficient than dry methods for synthesizing ferrite nanoparticles. They work at lower temperatures as compared to dry chemical methods and in the presence of solvents. According to scientists, wet chemical methods are better because they have the following advantages compared to dry methods.

1) Good shape and size control
2) Agglomeration control
3) Atomic-level control

The names of the different wet chemical methods are listed below [8]

I. Sol-Gel method
II. Co-precipitation Method
III. Microemulsion
IV. Hydrothermal Method
V. Sono-chemical Reaction
VI. Microwave Assisted
VII. Template synthesis
VIII. Gas/Vapor phase synthesis
IX. Spray pyrolysis
X. Oxidation-Reduction Method [9]

7. EXPERIMENTATION

2.1 Experimentation

There are various wet chemical methods available for the synthesis of ferrite Nanoparticles, the methods used for the present work are the Hydrothermal & Co-precipitation method because it is the simplest and cheapest way of producing the desired product.

Several experiments listed below were performed to carry out the specific objectives.

I. Preparation of $CuFe_2O_4$, $ZnFe_2O_4$ & Cu-$ZnFe_2O_4$ nanoparticles
II. Preparation of the core@shell structured $CuFe_2O_4$/$ZnFe_2O_4$/Cu-$ZnFe_2O_4$ @Al_2O_3 and $CuFe_2O_4$/$ZnFe_2O_4$/Cu-$ZnFe_2O_4$ @CuO total of six catalyst
III. Characteristics of the core@shell catalyst
IV. Reduction of p-nitro phenol using UV spectroscopy

2.1.1 Core formation $CuFe_2O_4$ /$ZnFe_2O_4$ /Cu-$ZnFe_2O_4$:

$CuFe_2O_4$ (Copper ferrite Spinel) was prepared using a hydrothermal process. The precursors used for the preparation of copper ferrite were Iron (II) Nitrate and Copper (II) Nitrate. 0.2M Iron nitrate and 0.1M copper nitrate were separately dissolved into 35 ml distilled water with a molar ratio of M3+/M2+ as 2:1 using a magnetic stirrer at room temperature to form aqueous iron nitrate (M1) and aqueous copper nitrate (M2) solutions. The aqueous solution was allowed to stir till the formation of a complete homogeneous solution. These solutions were then mixed to form a mixed solution (M3) and were kept on stirring at room temperature.

After that 6M NaOH (Sodium Hydroxide) aqueous solution (M4) was prepared within 10 ml of distilled water. This M4 solution was then quickly poured into the M3 solution while the M3 solution was still on the magnetic stirrer at room temperature. This new solution M5 was then stirred for a further 20 min at room temperature. This precipitated solution M5 is then sonicated for 20 min at room temperature. Then this whole mixture which is accompanied by 80 ml precipitated solution (35ml + 35ml + 10ml = 80ml) was shifted into the autoclave which was then sealed tightly and put into the laboratory oven at 160^oC for 12 h. Small stoichiometric amounts of the chemical were utilized due to limited autoclave capacity i.e., 100 ml.

In this 12 h process, Copper ferrite Nanoparticles were formed into the autoclave through a hydrothermal process. After this heating process in the laboratory oven, the oven was switched off and the autoclave was allowed to reach room temperature. The Nanocrystals formed were washed several times with distilled water till the pH becomes neutral and all basic media was removed from them. Then the Nanocrystals were put in a laboratory oven in a beaker at 160^oC for 12 h to dry.

After drying the solid nanoparticles were removed from the beaker and grinned to avoid agglomeration of the particles. These were the resultant $CuFe_2O_4$ nanoparticles. [10] [11] [12]

A similar Hydrothermal process was used for the formation of $ZnFe_2O$ & Cu-$ZnFe_2O_4$ nanoparticles synthesis. Hence total of three cores were synthesized in this experimental research work.

2.1.2 Alumina(Al_2O_3) coating/ Shell formation:

The co-precipitation method was used for Al_2O_3 (Alumina) coating of cores. A stoichiometric solution of 0.1M of $Al(NO_3)_3$ aluminum nitrate (M6) was formed in 100ml distilled water at room temperature using a magnetic stirrer. 0.1 gm of $CuFe_2O_4$ (copper ferrite)/ core (C1) was then added to the M6 solution and the temperature of the hot plate stirrer was raised to 60°C. In the meantime, precipitating agent, 1.5M sodium hydroxide solution (M7) was prepared and heated up to 60°C. M7 solution was then added to the M6 mixture to form M8 solution and heating was stopped while the mixture was kept on stirring for 1 h.

The resultant mixture M8 was allowed to settle down for the next 24 h. The alkaline decant was then removed from the top while the remaining mixture was washed several times till neutral pH of 7 was achieved. Then the sample was calcined in the furnace at 500°C for 10 h to form the final product. Similarly, zinc ferrite and Copper-Zinc mixed ferrites were also coated with alumina. [13]

2.1.3 CuO (Cupric Oxide) coating/ Shell formation:

The co-precipitation method was used for CuO (Cupric Oxide) coating of cores. A stoichiometric solution of 0.1M (M8) of $Cu(NO_3)_2$ copper nitrate was formed in 100ml distilled water at room temperature using a magnetic stirrer. 0.1gm $CuFe_2O_4$ (copper ferrite)/ core (C2) was then added to the M8 solution, and the temperature of the hot plate stirrer was raised to 60°C. In the meantime, 1.5M sodium hydroxide solution (M9) was prepared and heated up to 60°C. M9 solution was then added to M8 mixture to form M10 solution and heating was stopped while the mixture was kept on stirring for 1 h.

The resultant mixture M10 was allowed to settle down for the next 24 h. The decant was then removed from the top while the remaining mixture was washed several times till neutral pH of 7 was achieved. Similarly, zinc ferrite and Copper-Zinc mixed ferrites were also coated with cupric oxide [14]

8. RESULTS & DISCUSSION

3.1 Structural Analysis by XRD

Information about the crystalline phase and crystallite size of samples was obtained by using the XRD technique. Samples were scanned for 2ϴ range (20°-80°).

3.1.1 Structural Analysis of $CuFe_2O_4$, $ZnFe_2O_4$ & Cu-$ZnFe_2O_4$ (Cores)

Figure 2. shows the XRD patterns of $CuFe_2O_4$, $ZnFe_2O_4$ & Cu-$ZnFe_2O_4$ nanostructures prepared by using the hydrothermal technique. The broader XRD peak indicates that the particles have a small crystallite size and are in the Nanoscale range. Copper and Zinc ferrite comprised several peaks at 2θ values of 30.85 (d220), 35.30 (d311), 43.5 (d400), 53.80 (d422), 56.35 (d511), and 62.75 (d440) indicating a cubic crystal structure. These values of peaks were matched from standard cards, PDF#770010 for $CuFe_2O_4$ and PDF#221012 for $ZnFe_2O_4$ and it was found that all principal peaks were present in the result. These main peaks are shown with green vertical lines. All these phases were present in all three ferrites which indicates that copper and zinc ferrites were successfully prepared. After attaining these satisfactory results, the ferrites were then coated to proceed with the study.

Some impurities were also found in the samples. These impurities are marked with an "*" asterisk sign. These peaks are of CuO. These CuO peaks were matched with standard card PDF#450937. These impurities did not affect the shell formation process neither they affected the kinetics study. In most of the recent research work, these peaks were present.

The crystallite sizes were calculated by using shrerre's equation. Their sizes were in the following ranges.

- $CuFe_2O_4$ = 4.91 – 19.54 nm
- $ZnFe_2O_4$ = 3.16 – 8.44 nm
- Cu-$ZnFe_2O_4$ = 5.37 – 8.43 nm

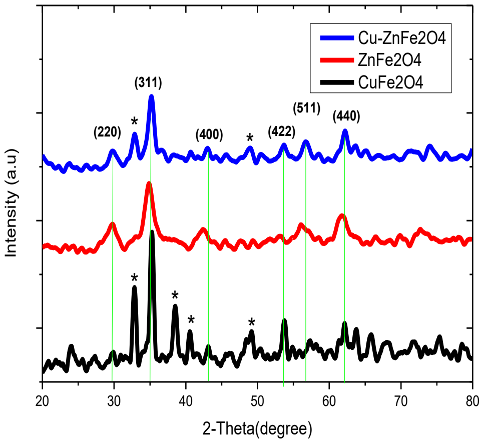

Fig. 2. XRD patterns of $CuFe_2O_4$, $ZnFe_2O_4$ & Cu-$ZnFe_2O_4$ nanostructures

3.1.2 Structural Analysis of $CuFe_2O_4$/CuO, $ZnFe_2O_4$ /CuO, Cu-$ZnFe_2O_4$ /CuO

Figure 3 shows the XRD patterns of pure $CuFe_2O_4$/CuO, $ZnFe_2O_4$ /CuO, and Cu-$ZnFe_2O_4$ /CuO nanostructures prepared by using the co-precipitation technique. Copper oxide comprised several peaks at 2θ values of 33.85 (d_{-110}), 35.55 (d_{-111}), 39.10 (d_{111}), 48.50 (d_{-202}), 53.45 (d_{020}), 57.25 (d_{202}), 61.20 (d_{-113}), 66.20 (d_{022}) and 67.02 (d_{-220}) indicating a monoclinic crystal structure. These values of peaks were matched from standard cards, PDF#450937 of CuO and it was found that all principal peaks were present in the result. These main peaks are shown with green vertical lines. All these phases were present in all three samples which indicates that copper oxide coating was successfully done.

Some impurities were also found in the samples. These impurities are marked with a "+" plus sign. These peaks are of base material i.e., copper and zinc ferrites. These impurity peaks were matched with standard card PDF#770010 for $CuFe_2O_4$ and PDF#221012 for $ZnFe_2O_4$. These impurities did not affect the shell formation process neither they affected the kinetics study. Also, only two base peaks were present which shows that good coating was done.

The crystallite sizes were calculated by using shrerre's equation. Their sizes were in the following ranges.

- $CuFe_2O_4$ /CuO = 5.03 – 12.14 nm

- $ZnFe_2O_4$ /CuO = 8.71 – 12.13 nm
- Cu-$ZnFe_2O_4$ /CuO = 4.29 – 8.53 nm

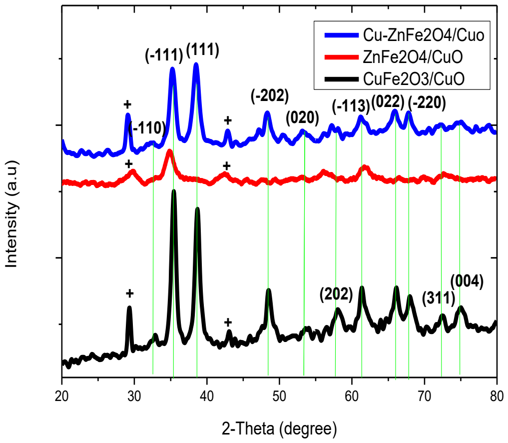

Fig. 3. XRD patterns of pure $CuFe_2O_4$/CuO, $ZnFe_2O_4$ /CuO, and Cu-$ZnFe_2O_4$ /CuO nanostructures

3.1.3 Structural Analysis of $CuFe_2O_4/Al_2O_3$, $ZnFe_2O_4/Al_2O_3$, Cu-$ZnFe_2O_4$ /Al_2O_3

Figure 4. shows the XRD patterns of pure $CuFe_2O_4/Al_2O_3$, $ZnFe_2O_4$/ Al_2O_3, and Cu-$ZnFe_2O_4$ /Al_2O_3 nanostructures prepared by the co-precipitation technique. Alumina Al_2O_3 comprised several peaks at 2θ values of 35.50 (d_{104}), 39.90 (d_{110}), 44.02 (d_{113}), 54.50 (d_{024}), 57.20 (d_{116}), 63.20 (d_{214}) indicating a hexagonal crystal structure.

These values of peaks were matched from standard cards, PDF#82146 of Al_2O_3 and it was found that all principal peaks were present in the result. All these phases were present in all three samples which indicates that alumina coating was successfully done.

Some impurities were also found in the samples. These impurities are marked with a "+" plus & "*" asterisk sign. "+" peaks are of base material i.e., copper and zinc ferrites and "*" peaks are of copper oxide which is too base or core material. These impurity peaks were matched with standard card PDF#770010 for $CuFe_2O_4$, PDF#221012 for $ZnFe_2O_4$, and PDF#450937 for CuO. These impurities did not affect the kinetics study. Four impurity peaks were present which indicates two things, whether the shell is not completely formed, or alumina thickness is very thin, and X-rays have transmitted through the coated surface and also showed base or core material also. The latter part has more significant chances because the previously reported result shows that the alumina coating is very thin. Hence it can be assumed that shell formation has been done successfully but the coating thickness is very thin.

The crystallite sizes were calculated by using shrerre's equation. Their sizes were in the following ranges.

- $CuFe_2O_4$ /Al_2O_3 = 12.77 – 25.21 nm
- $ZnFe_2O_4$ /Al_2O_3 = 11.6 – 17.73 nm
- Cu-$ZnFe_2O_4$/Al_2O_3 =11.63 – 17.84 nm

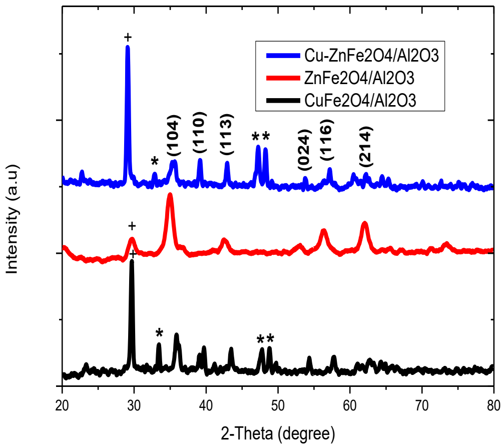

Fig. 4. XRD patterns of pure $CuFe_2O_4/Al_2O_3$, $ZnFe_2O_4$/ Al_2O_3, and Cu-$ZnFe_2O_4$ /Al_2O_3 nanostructures

3.2 Morphological Analysis by SEM

Morphological analysis of synthesized ferrites was carried out by using scanning electron microscopy.

SEM provides information on particle size and morphology. Prior to morphological analysis under scanning electron microscopy, the dispersion was prepared by sonicating the ferrite in distilled water for 2 hours. A few drops of the dispersion were dropped onto a slide and dried under a lamp, and the slide was analyzed. The ferrite was analyzed under a scanning electron microscope and the magnification was in the range of X50,000. From the micrographs of $CuFe_2O_4$ (in Figure 5 it can be seen that the particles are uniformly dispersed and cubical. The core/ shell particles of $CuFe_2O_4$@CuO & $CuFe_2O_4@Al_2O_3$ were also found to be in the range of 11 ± 2 nm to 25 ± 2 nm. Coated sample micrographs show that the particles are unagglomerated. One application of the coating is that it reduces agglomeration which is clearly shown by these micrographs. This particle size range was well consistent with XRD results. The table below shows the Energy dispersive X-ray analysis (EDX) of copper ferrite which was used to determine the chemical composition of the as-prepared ferrite products. Results of EDX show that the sample contains O, Cu, and Fe only. Their atomic percentages are also shown.

The micrographs of $ZnFe_2O_4$ (in Figure 6) show that the particles are uniformly dispersed and spherical. The core/ shell particles of $ZnFe_2O_4$@CuO & $ZnFe_2O_4@Al_2O_3$ were also found to be in the range of 8 ± 2 nm to 45 ± 2 nm. This particle size range was well consistent with XRD results. Coated sample micrographs show that the particles are unagglomerated. The table below shows the Energy dispersive X-ray analysis (EDX) of Zinc ferrite which was used to determine the chemical composition of the as-prepared ferrite products. Results of EDX show that the sample contains O, Zn, and Fe only. Their atomic percentages are also shown.

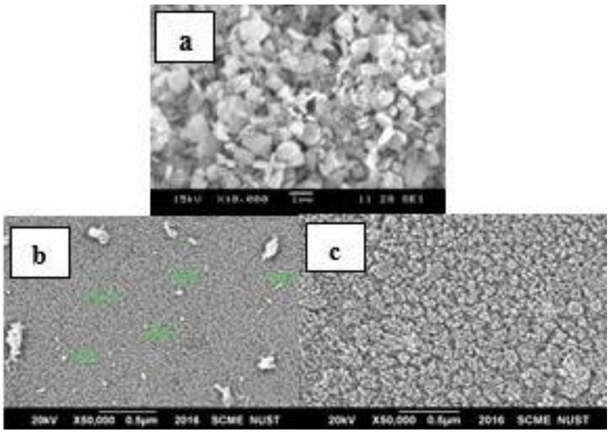

Fig. 5. SEM photographs of (a) $CuFe_2O_4$,(b) $CuFe_2O_4@CuO$, (c) $CuFe_2O_4@Al_2O_3$

Table 1. EDX determined atomic composition of $CuFe_2O_4$

Element	Mass %	Atomic %
O K	17.54	45.10
Cu K	62.75	40.33
Fe K	19.72	14.40
Total	100.00	100.00

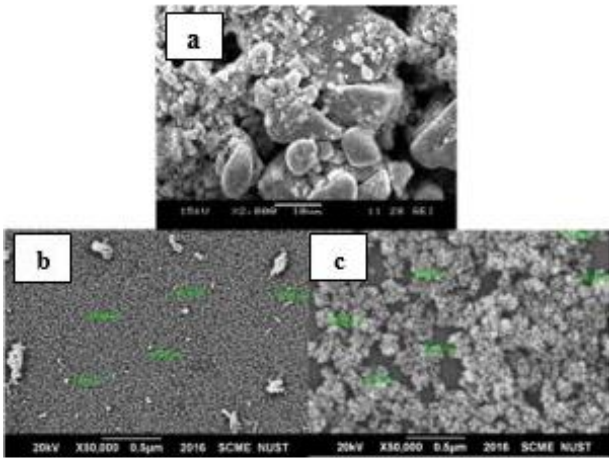

Fig. 6. SEM photographs of (a) $ZnFe_2O_4$, (b) $ZnFe_2O_4@CuO$, (c) $ZnFe_2O_4@Al_2O_3$

Table 2. EDX determined atomic composition of $ZnFe_2O_4$

Element	Mass %	Atomic %
O K	14.31	38.01
Zn K	32.09	20.90
Fe K	53.60	41.02
Total	100.00	100.00

The micrographs of $Cu-ZnFe_2O_4$ (in Figure 7) shows that the particles are uniformly dispersed and crystal and spherical mix shaped. The core/ shell particles of $Cu-ZnFe_2O_4@CuO$ &$Cu- ZnFe_2O_4@Al_2O_3$ were found to be in the range of 16 ± 2 nm to 40 ± 2 nm. This particle size range was well consistent with XRD results. Coated sample micrographs show that the particles are unagglomerated. The table below shows the Energy dispersive X-ray analysis (EDX) of copper-zinc ferrite which was used to determine the chemical composition of the as-prepared ferrite products. Results of EDX show that the sample contains O, Zn, Cu, and Fe only. Their percentages are also shown.

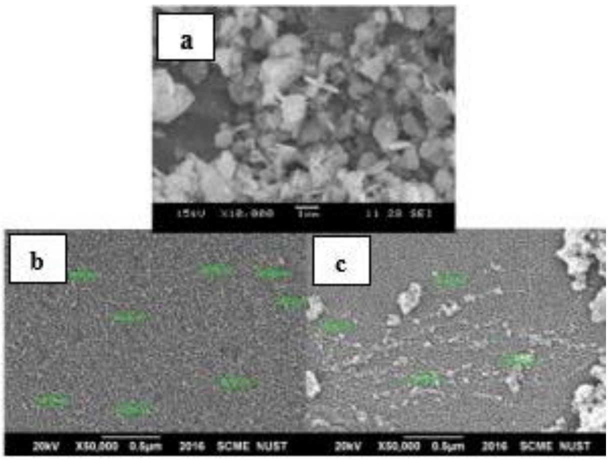

Fig. 7. SEM photographs of (a) $Cu-ZnFe_2O_4$, (b) $Cu-ZnFe_2O_4@CuO$, (c) $Cu-ZnFe_2O_4@Al_2O_3$

Table 3. EDX determined the atomic composition of $Cu-ZnFe_2O_4$

Element	Mass %	Atomic %
O K	10.15	30.28
Cu K	30.23	24.71
Zn K	35.30	25.96
Fe K	24.32	20.91
Total	100.00	100.00

3.3 Catalytic degradation of Para-Nitro phenol

The catalytic degradation of para-nitrophenol was determined by the core/shell nanostructure using UV-Visible spectrophotometry. The aqueous solution of p-nitrophenol was mixed with an aqueous solution of sodium borohydride. Sodium borohydride was used as the reducing agent. The degradation reaction was monitored by using a UV-Vis spectrophotometer. The degradation reaction was monitored in the spectral range of 200 nm to 500 nm. The UV-Vis spectra for the degradation reaction are shown in Figures 8.1-8.6. The degradation reaction started in the presence of a catalyst. Samples were taken and analyzed at regular intervals. Spectra obtained by UV-Vis spectroscopy of p-nitro phenol aqueous solution showed that nitro phenol exhibited absorbance at 317 nm. When an aqueous solution of p-nitro phenol was mixed with an aqueous solution of sodium borohydride, the peak was shifted to 401 nm for an instance, which shifted back to 317 nm when the catalyst was added. When core/ shell ferrite was added, the degradation reaction was initiated. The results are as follows:

$CuFe_2O_4$/ $ZnFe_2O_4$ & $Cu-ZnFe_2O_4@CuO/Al_2O_3$ all can be used as a catalyst for the degradation of p-nitro phenol. With respect to time the catalytic reactions can be divided in two categories. In first place there comes Copper Ferrites and mix ferrites which achieved maximum conversion in 25 min. while the rest of them achieved max conversion in 40-45 min

3.4 Kinetics of a photochemical reaction

To find out the kinetics (n, k) of degradation reaction, different methods can be utilized, like integral and differential methods. Differential method of analysis has been chosen to find the kinetic parameters for the degradation reaction of p-nitrophenol. The relationship between the absorbance (D) and the concentration (C) during the reaction is given by;

$$C_o = \mathcal{E}(D_\infty - D_o) \qquad (1)$$

$$C = \mathcal{E}(D_\infty - D) \qquad (2)$$

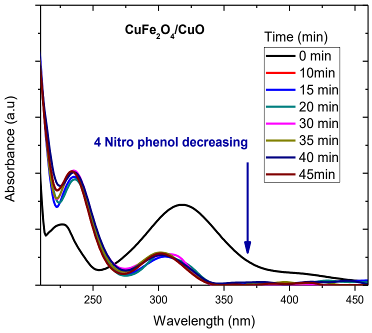

Fig. 8.1 UV-Visible spectra of $CuFe_2O_4$@CuO

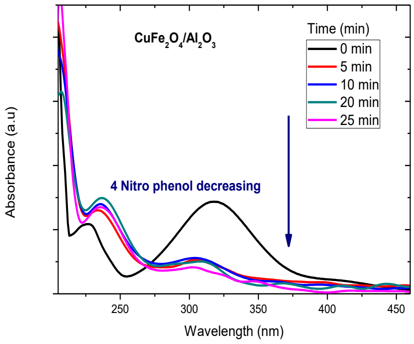

Fig. 8.2 UV-Visible spectra of $CuFe_2O_4$@Al_2O_3

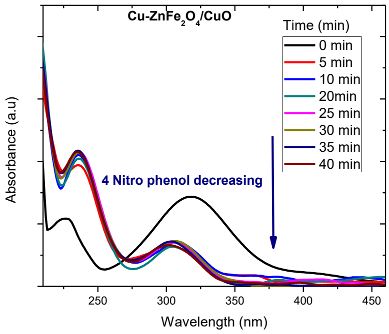

Fig. 8.3 UV-Visible spectra of Cu-$ZnFe_2O_4$@CuO

where C_0 is the concentration at time t = 0, C is the concentration at any time, and Ɛ is molar absorption coefficients at a specified wavelength. Substituting above equations in Langmuir-Hinshelwood model.

$$-\ln \frac{C_{Af}}{C_{A0}} = kt \qquad (3)$$

$$\ln(D_\infty - D) = -kt + \ln(D_\infty - D) \qquad (4)$$

$$D_\infty - D = (D_\infty - D)e^{-kt} \qquad (5)$$

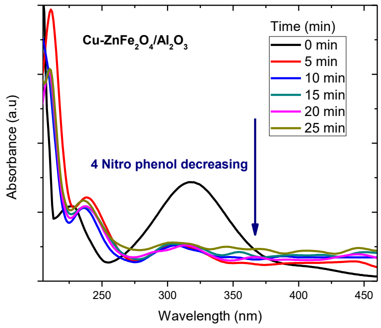

Fig. 8.4 UV-Visible spectra of Cu-$ZnFe_2O_4$@Al_2O_3

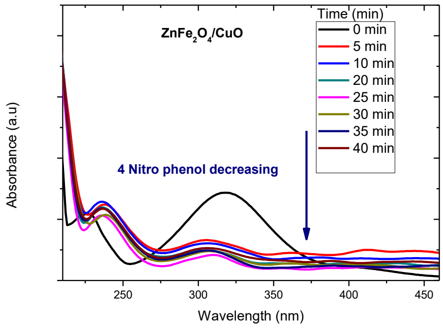

Fig. 8.5 UV-Visible spectra of $ZnFe_2O_4$@CuO

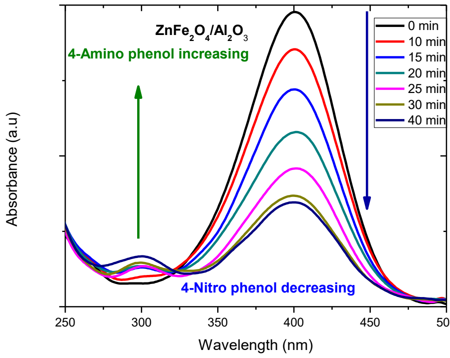

Fig. 8.6 UV-Visible spectra of $ZnFe_2O_4$@Al_2O_3

Table 4. Percentage Catalytic activity of synthesized catalysts

Catalyst	% Conversion
$CuFe_2O_4$/CuO	70.67
$CuFe_2O_4$/Al_2O_3	73.33
Cu-$ZnFe_2O_4$/CuO	66.67
Cu-$ZnFe_2O_4$/Al_2O_3	66.67
Zn Fe_2O_4/CuO	**80.00**
$ZnFe_2O_4$/Al_2O_3	72.50

The above equation reveals that the absorbance tends to the value as that of expression in terms of concentration after the completion of a reaction (infinite time). The rate constant can be found by the slope of ln (D_∞ - D_0) vs time graph. The same equation can be expressed in terms of concentration. For all catalysts, on an average, Order of the reaction was 2.55 while rate constant value was 8.555 min^{-1} whereas for $ZnFe_2O_4@Al_2O_3$, 1st order kinetics was observed.

To compare the performance of the catalyst their % conversion was calculated.

$$\% \text{ Conversion} = \frac{C_0 - C}{C_0} \times 100 \qquad (6)$$

It can be concluded that the % catalytic conversion can be divided into 3 zones. In first place comes Zinc ferrites with maximum conversion of 80% in 40 min. In second place Copper ferrites with 70-73 % conversion while in third place there comes mix ferrites which gave least conversions of 66.67%.

9. CONCLUSION

Magnetic $CuFe_2O_4$ / $ZnFe_2O_4$ / Cu-$ZnFe_2O_4$ were prepared by using hydrothermal method and were coated with Al_2O_3 and CuO respectively by using co-precipitation method. The characteristics of as synthesized nano-catalyst was examined by using different techniques such as X-ray diffraction (XRD), scanning electron microscope (SEM), energy dispersive X-ray analysis (EDXA) and UV–visible spectroscopy. The XRD patterns confirms the formation of $CuFe_2O_4$ / Zn Fe_2O_4 / Cu-$ZnFe_2O_4$ @ Al_2O_3 / CuO nano-catalyst. The boarder peaks of XRD patterns confirms that the particles are in nanoscale. The morphology analysis was done by using the SEM. The morphological analysis reveals that the nano-sized particles are homogeneous, uniformly distributed and less agglomerated nanoparticles. Average size particle was found in the range of 8±2 nm to 45±2 nm. EDX analysis of core material shows composition and mass percentages of constituting elements. It confirms the presence of Cu, Fe, Zn and O atoms. The synthesized nano-catalyst were applied for the reduction of Para-nitro phenol with excess sodium borohydride. As evidence from the UV spectra, the synthesized nano-catalyst successfully reduced the Para-nitro phenol with catalytic efficiency of 80.00%.

5. REFERENCES

[1] M. M. Baig, Erum Pervaiz, M. J. Afzal, “Catalytic Activity and Kinetic Studies of Core@Shell Nanostructure $NiFe_2O_4@TiO_2$ for Photocatalytic Degradation of Methyl Orange Dye”

[2] B. I. Kharisov, "Mini-review : Ferrite nanoparticles in the catalysis," Arab. J. Chem, 2014.

[3] Ankita Goyal, S. Bansal, Sonal Singhal,"Facile reduction of nitrophenols: Comparative catalytic efficiency of MFe2O4 (M = Ni, Cu, Zn) nanoferrites," international journal of hydrogen energy, vol. 39, pp. 4895-4908, (2014).

[4] Jie Feng, Li Sua, Yanhua Maa, Cuiling Ren, Qing Guo, Xingguo Chen, "CuFe2O4 magnetic nanoparticles: A simple and efficient catalyst for the reduction of nitrophenol," Chemical Engineering Journal, vol. 221, p. 16–24, 2013

[5] K. Byrappa, Masahiro Yoshimura,"Handbook of Hydrothermal Technology, The Boulevard, Langford Lane, Kidlington, Oxford: Elsevier Inc., 2013.

[6] Paria, R. G, ", “Core / Shell Nanoparticles : Classes , Properties ,Synthesis Mechanisms , Characterization , and Applications," vol. 1, p. 2373–2433, 2012.

[7] E. Casbeer, V. K. Sharma, and X. Li, "Synthesis and photocatalytic activity of ferrites under visible light : A review," Sep. Purif. Technol, vol. 87, p. 1–14, 2012.

[8] Z. Karimi, L. K, "Nano-magnetic particles used in biomedicine : Core and coating materials," Mater. Sci. Eng. C, Vols. 33, no. 5, p. 2465–2475, 2013.

[9] A. I. Kirkland and J. L. Hutchison, "Nanocharacterisation,"," Vols. vol. 1,, 2007.

[10] Jie Feng, Li Sua, Yanhua Maa, Cuiling Ren, Qing Guo, Xingguo Chen, "CuFe2O4 magnetic nanoparticles: A simple and efficient catalyst for the reduction of nitrophenol," Chemical Engineering Journal, vol. 221, p. 16–24, 2013.

[11] Hongxiao Zhao, Huimin Jia, Shumin Wang, Dengqi Xue "Fabrication and application of MFe2O4 (M = Zn, Cu) nanoparticles as anodes for Li ion batteries," Journal of Experimental Nanoscience, vol. 6:1, pp. 75-83, 2011.

[12] Hong Deng∗, Hongyu Chen, He Li, "Synthesis of crystal MFe2O4 (M = Mg, Cu, Ni) microspheres," Materials Chemistry and Physics, vol. 101, p. 509–513, 2007.

[13] Hankarea, "Enhanced photocatalytic degradation of methyl red and thymol blue using titania–alumina–zinc ferrite nanocomposite," Applied Catalysis B: Environmental, vol. 107, p. 333– 339, 2011.

[14] Jiajia Ding, Lizhong Liu, Jinjuan Xue, Zhengwei Zhou, Guangyu He, Haiqun Chen "Low-temperture preparation of magnetically separable Fe3O4@CuO-RGO core-shell heterojunctions for high-perfomance removal of organic dye under visible light," Journal of Alloys and Compounds, vol. JALCOM 38169, p. 25, 2016.